

Leak-rate of seals: comparison of theory with experiment

B. Lorenz and B.N.J. Persson
IFF, FZ Jülich, D-52425 Jülich, Germany

Seals are extremely useful devices to prevent fluid leakage. We present experimental results for the leak-rate of rubber seals, and compare the results to a novel theory, which is based on percolation theory and a recently developed contact mechanics theory. We find good agreement between theory and experiment.

A seal is a device for closing a gap or making a joint fluid tight[1]. Seals play a crucial role in many modern engineering devices, and the failure of seals may result in catastrophic events, such as the Challenger disaster. In spite of its apparent simplicity, it is not easy to predict the leak-rate and (for dynamic seals) the friction forces[2] for seals. The main problem is the influence of surface roughness on the contact mechanics at the seal-substrate interface. Most surfaces of engineering interest have surface roughness on a wide range of length scales[3], e.g, from cm to nm, which will influence the leak rate and friction of seals, and accounting for the whole range of surface roughness is impossible using standard numerical methods, such as the Finite Element Method.

In this paper we present experimental results for the leak-rate of rubber seals, and compare the results to a novel theory[3, 4, 5], which is based on percolation theory and a recently developed contact mechanics theory[6, 7, 8, 9, 10, 11, 12], which accurately takes into account the elastic coupling between the contact regions in the nominal rubber-substrate contact area. Earlier contact mechanics models, such as the Greenwood–Williamson[13] model or the model of Bush et al[14], neglect this elastic coupling, which results in highly incorrect results[15, 16], in particular for the relations between the squeezing pressure and the interfacial separation[17]. We assume that purely elastic deformation occurs in the

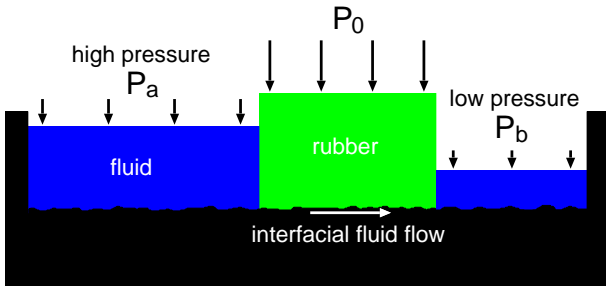


FIG. 1: Rubber seal (schematic). The liquid on the left-hand-side is under the hydrostatic pressure P_a and the liquid to the right under the pressure P_b (usually, P_b is the atmospheric pressure). The pressure difference $\Delta P = P_a - P_b$ results in liquid flow at the interface between the rubber seal and the rough substrate surface. The volume of liquid flow per unit time is denoted by \dot{Q} , and depends on the squeezing pressure P_0 acting on the rubber seal.

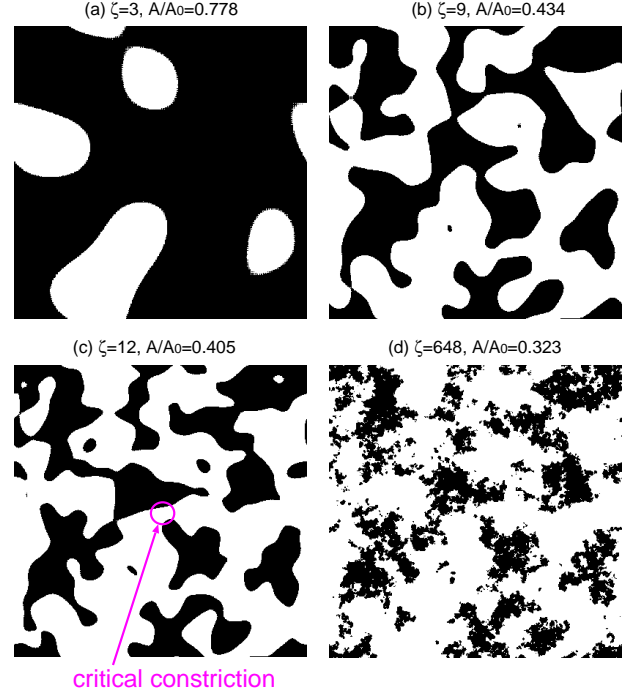


FIG. 2: The contact region at different magnifications $\zeta = 3, 9, 12$ and 648 , are shown in (a)-(d) respectively. When the magnification increases from 9 to 12 the non-contact region percolate. At the lowest magnification $\zeta = 1$: $A(1) = A_0$. The figure is the result of Molecular Dynamics simulations of the contact between elastic solids with randomly rough surfaces, see Ref. [5].

solids, which is the case for rubber seals.

Consider the fluid leakage through a rubber seal, from a high fluid pressure P_a region, to a low fluid pressure P_b region, as in Fig. 1. Assume that the nominal contact region between the rubber and the hard countersurface is rectangular with area $L_x \times L_y$. We assume that the high pressure fluid region is for $x < 0$ and the low pressure region for $x > L_x$. We “divide” the contact region into squares with the side $L_x = L$ and the area $A_0 = L^2$ (this assumes that $N = L_y/L_x$ is an integer, but this restriction does not affect the final result). Now, let us study the contact between the two solids within one of the squares as we change the magnification ζ . We define $\zeta = L/\lambda$, where λ is the resolution. We study how the

apparent contact area (projected on the xy -plane), $A(\zeta)$, between the two solids depends on the magnification ζ . At the lowest magnification we cannot observe any surface roughness, and the contact between the solids appears to be complete i.e., $A(1) = A_0$. As we increase the magnification we will observe some interfacial roughness, and the (apparent) contact area will decrease. At high enough magnification, say $\zeta = \zeta_c$, a percolating path of non-contact area will be observed for the first time, see Fig. 2. We denote the most narrow (and least high) constriction along this percolation path as the *critical constriction*. The critical constriction will have the lateral size $\lambda_c = L/\zeta_c$ and the surface separation at this point is denoted by u_c . We can calculate $u_c \approx u_1(\zeta_c)$, using a recently developed contact mechanics theory[11]. Thus, we define $u_1(\zeta)$ to be the (average) height separating the surfaces which appear to come into contact when the magnification decreases from ζ to $\zeta - \Delta\zeta$, where $\Delta\zeta$ is a small (infinitesimal) change in the magnification. $u_1(\zeta)$ can be calculated as described below. As we continue to increase the magnification we will find more percolating channels between the surfaces, but these will have more narrow constrictions than the first channel which appears at $\zeta = \zeta_c$, and as a first approximation we will neglect the contribution to the leak-rate from these channels[5].

A first rough estimate of the leak-rate is obtained by assuming that all the leakage occurs through the critical percolation channel, and that the whole pressure drop $\Delta P = P_a - P_b$ (where P_a and P_b is the pressure to the left and right of the seal) occurs over the critical constriction [of width and length $\lambda_c \approx L/\zeta_c$ and height $u_c = u_1(\zeta_c)$]. If we approximate the critical constriction as a pore with rectangular cross section (width and length λ_c and height $u_c \ll \lambda_c$), and if assume an incompressible Newtonian fluid, the volume-flow per unit time through the critical constriction will be given by (Poiseuille flow)

$$\dot{Q} = \alpha \frac{u_1^3(\zeta_c)}{12\eta} \Delta P, \quad (1)$$

where η is the fluid viscosity. In deriving (1) we have assumed laminar flow and that $u_c \ll \lambda_c$, which is always satisfied in practice. We have also assumed no-slip boundary condition on the solid walls. This assumption is not always satisfied at the micro or nano-scale, but is likely to be a very good approximation in the present case owing to surface roughness which occurs at length-scales shorter than the size of the critical constriction.

In (1) we have introduced a factor α which depends on the exact shape of the critical constriction, but which is expected to be of order unity. The flow rate expected for a channel with rectangular cross section (height u_1 and width and length λ_c with $u_1 \ll \lambda_c$) correspond to $\alpha = 1$. However, the actual flow channel will not have a rectangular cross section but the pore height must go continuously to zero at the “edges” in the direction

perpendicular to the fluid flow. In addition, the channel is of course not exactly rectangular in the xy -plane, and this too will effect α . Note also that a given percolation channel could have several narrow (critical or nearly critical) constrictions of nearly the same dimension which would reduce the flow along the channel. But in this case one would also expect more channels from the high to the low fluid pressure side of the junction, which would tend to increase the leak rate. These two effects will, at least in the simplest picture, compensate each other (see discussion in Ref. [5]). Finally, since there are $N = L_y/L_x$ square areas in the rubber-countersurface (apparent) contact area, we get the total leak-rate

$$\dot{Q} = \alpha \frac{L_y}{L_x} \frac{u_1^3(\zeta_c)}{12\eta} \Delta P. \quad (2)$$

To complete the theory we must calculate the separation $u_c = u_1(\zeta_c)$ of the surfaces at the critical constriction. We first determine the critical magnification ζ_c by assuming that the apparent relative contact area at this point is given by site percolation theory. Thus, the relative contact area $A(\zeta)/A_0 \approx 1 - p_c$, where p_c is the so called site percolation threshold[18]. For an infinite-sized systems $p_c \approx 0.696$ for a hexagonal lattice and 0.593 for a square lattice[18]. For finite sized systems the percolation will, on the average, occur for (slightly) smaller values of p , and fluctuations in the percolation threshold will occur between different realizations of the same physical system. We take $p_c \approx 0.6$ so that $A(\zeta_c)/A_0 \approx 0.4$ will determine the critical magnification $\zeta = \zeta_c$.

The (apparent) relative contact area $A(\zeta)/A_0$ at the magnification ζ can be obtained using the contact mechanics formalism developed elsewhere[6, 8, 9, 10, 11], where the system is studied at different magnifications ζ . We have[6, 7]

$$\frac{A(\zeta)}{A_0} = \frac{1}{(\pi G)^{1/2}} \int_0^{P_0} d\sigma e^{-\sigma^2/4G} = \text{erf} \left(\frac{P_0}{2G^{1/2}} \right)$$

where

$$G(\zeta) = \frac{\pi}{4} \left(\frac{E}{1-\nu^2} \right)^2 \int_{q_0}^{\zeta q_0} dq q^3 C(q)$$

where the surface roughness power spectrum

$$C(q) = \frac{1}{(2\pi)^2} \int d^2x \langle h(\mathbf{x})h(\mathbf{0}) \rangle e^{-i\mathbf{q} \cdot \mathbf{x}}$$

where $\langle \dots \rangle$ stands for ensemble average. Here E and ν are the Young's elastic modulus and the Poisson ratio of the rubber. The height profile $h(\mathbf{x})$ of the rough surface can be measured routinely today on all relevant length scales using optical and stylus experiments.

We define $u_1(\zeta)$ to be the (average) height separating the surfaces which appear to come into contact when the

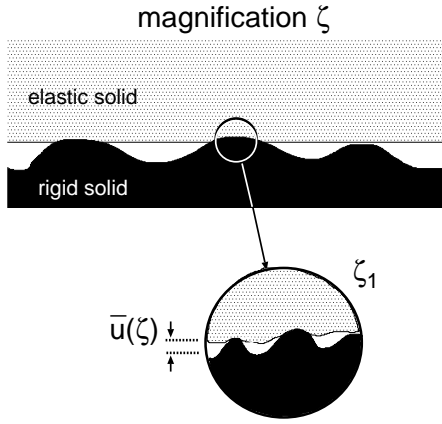


FIG. 3: An asperity contact region observed at the magnification ζ . It appears that complete contact occur in the asperity contact region, but when the magnification is increasing to the highest (atomic scale) magnification ζ_1 , it is observed that the solids are actually separated by the average distance $\bar{u}(\zeta)$.

magnification decreases from ζ to $\zeta - \Delta\zeta$, where $\Delta\zeta$ is a small (infinitesimal) change in the magnification. $u_1(\zeta)$ is a monotonically decreasing function of ζ , and can be calculated from the average interfacial separation $\bar{u}(\zeta)$ and $A(\zeta)$ using (see Ref. [11])

$$u_1(\zeta) = \bar{u}(\zeta) + \bar{u}'(\zeta)A(\zeta)/A'(\zeta).$$

The quantity $\bar{u}(\zeta)$ is the average separation between the surfaces in the apparent contact regions observed at the magnification ζ , see Fig. 3. It can be calculated from [11]

$$\bar{u}(\zeta) = \sqrt{\pi} \int_{\zeta q_0}^{q_1} dq q^2 C(q) w(q) \int_{p(\zeta)}^{\infty} dp' \frac{1}{p'} e^{-[w(q,\zeta)p'/E^*]^2},$$

where $p(\zeta) = P_0 A_0 / A(\zeta)$ and

$$w(q, \zeta) = \left(\pi \int_{\zeta q_0}^q dq' q'^3 C(q') \right)^{-1/2}.$$

The function $P(q, p, \zeta)$ is given by

$$P(q, p, \zeta) = \frac{2}{\sqrt{\pi}} \int_0^{s(q,\zeta)p} dx e^{-x^2},$$

where $s(q, \zeta) = w(q, \zeta)/E^*$.

We have performed a very simple experiment to test the theory presented above. In Fig. 4 we show our set-up for measuring the leak-rate of seals. A glass (or PMMA) cylinder with a rubber ring (with rectangular cross-section) attached to one end is squeezed against a hard substrate with well-defined surface roughness. The cylinder is filled with water, and the leak-rate of the fluid at the rubber-countersurface is detected by the change in the height of the fluid in the cylinder. In this case the pressure difference $\Delta P = P_a - P_b = \rho g H$, where g is the gravitation constant, ρ the fluid density and

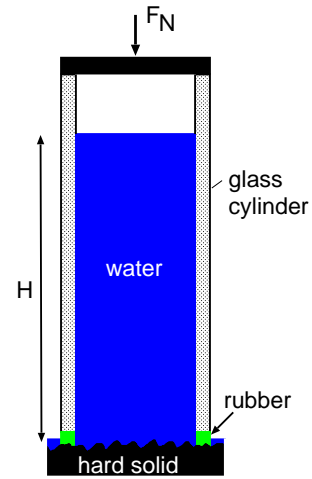


FIG. 4: Experimental set-up for measuring the leak-rate of seals. A glass (or PMMA) cylinder with a rubber ring attached to one end is squeezed against a hard substrate with well-defined surface roughness. The cylinder is filled with water, and the leak-rate of the water at the rubber-countersurface is detected by the change in the height of the water in the cylinder.

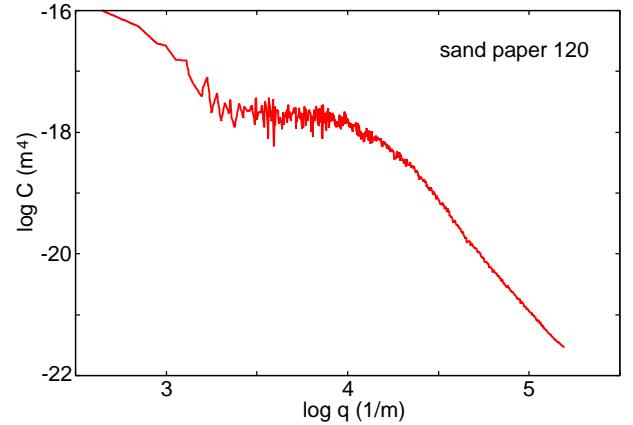


FIG. 5: Surface roughness power spectrum of sand paper 120. The surface has the root-mean-square roughness $44 \mu\text{m}$ and the surface area (including only the surface roughness with wavelength above $\lambda_1 = 20 \mu\text{m}$) is about 40% larger than the nominal surface area A_0 (i.e., the surface area projected on the xy -plane).

H the height of the fluid column. With $H \approx 1 \text{ m}$ we get typically $\Delta P \approx 0.01 \text{ MPa}$. With the diameter of the glass cylinder of order a few cm, the condition $P_0 \gg \Delta P$ (which is necessary in order to be able to neglect the influence on the contact mechanics from the fluid pressure at the rubber-countersurface) is satisfied already for loads (at the upper surface of the cylinder) of order kg. In our study we use a rubber ring with the Young's elastic modulus $E = 2.3 \text{ MPa}$, and with the inner and outer diameter 3 cm and 4 cm, respec-

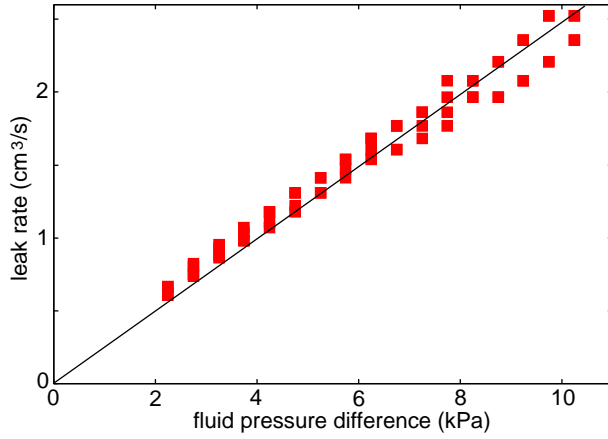


FIG. 6: Square symbols: the measured leak rate for different fluid pressure drop $\Delta P = P_a - P_b$ for the nominal squeezing pressure $P_0 \approx 60$ kPa.

tively, and the height 0.5 cm. The rubber ring was made from a silicon elastomer (PDMS) prepared using a two-component kit (Sylgard 184) purchased from Dow Corning (Midland, MI). The kit consist of a base (vinyl-terminated polydimethylsiloxane) and a curing agent (methylhydrosiloxane-dimethylsiloxane copolymer) with a suitable catalyst. From these two components we prepared a mixture 10:1 (base/cross linker) in weight. The mixture was degassed to remove the trapped air induced by stirring from the mixing process and then poured into casts. The bottom of these casts was made from glass to obtain smooth surfaces. The samples were cured in an oven at 80°C for 12 h. The substrate is a corundum paper (grit size 120) with the root-mean-square roughness 44 μm . From the measured surface topography we obtain the surface roughness power spectrum $C(q)$ shown in Fig. 5.

According to (1) we expect the leak-rate to increase linearly with the fluid pressure difference $\Delta P = P_a - P_b$. We first performed some experiments to test this prediction. In Fig. 6 we show the measured leak rate for different fluid pressure drop ΔP for the nominal squeezing pressure $P_0 \approx 60$ kPa. To within the accuracy of the experiment, the leak-rate depends linearly on ΔP .

In Fig. 7 we show the measured leak rate for ten different squeezing pressures (square symbols). The solid line is the calculated leak rate using the measured rubber elastic modulus $E = 2.3$ MPa and the surface power spectrum $C(q)$ shown in Fig. 5. In Fig. 8 we show the same as in Fig. 7 but for a logarithmic (with 10 as basis) leak-rate scale.

In Fig. 9 we show the calculated critical pore size as a function of the squeezing pressure. Note that the height of the critical pore is about 10 times smaller than the lateral size of the pore. Finally, in Fig. 10 we show the critical magnification ζ_c , where the non-contact area percolate, as a function of the squeezing pressure. Note

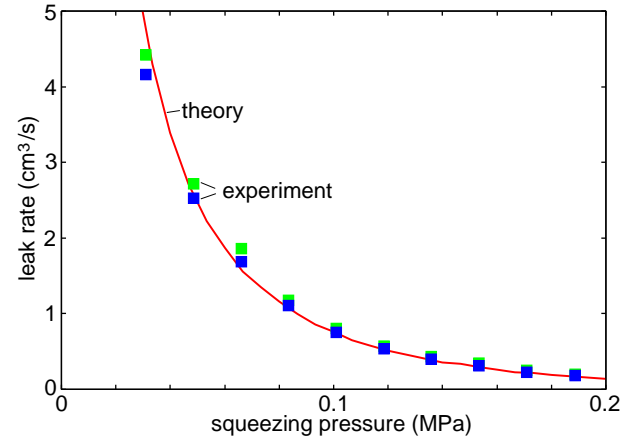


FIG. 7: Square symbols: the measured leak rate for ten different squeezing pressures. The experiment was performed twice, corresponding to the two data points for each pressure. Solid line: the calculated leak rate using the measured surface topography, the measured rubber elastic modulus $E = 2.3$ MPa and the fluid pressure difference $\Delta P = P_a - P_b = 10$ kPa obtained from the height of the water column. We have used $\alpha = 0.2$.

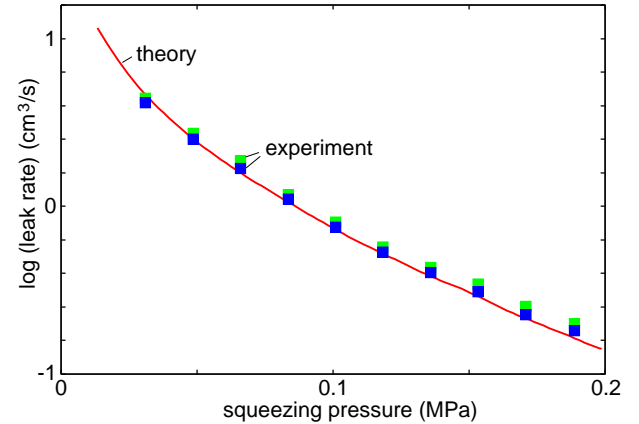


FIG. 8: The same as in Fig. 7 but for a logarithmic (with 10 as basis) leak-rate scale.

that, as expected, the percolation of the non-contact area occur at higher and higher magnification as the squeezing pressure increases.

Sand paper has much sharper and larger roughness than the counter surface used in normal rubber seal applications. However, from a theory point of view it should not really matter on which length scale the roughness occurs, except for “complications” such as the influence of adhesion and fluid contamination particles (which tend to clog the flow channels). Nevertheless, the theory assumes that the average surface slope is not too large and we plan to measure the leak rate for rubber seal in contact with sand blasted Plexiglas with a root-mean-square roughness in the micrometer range. Our initial experiment with Plexiglas showed that the leak rate decreased

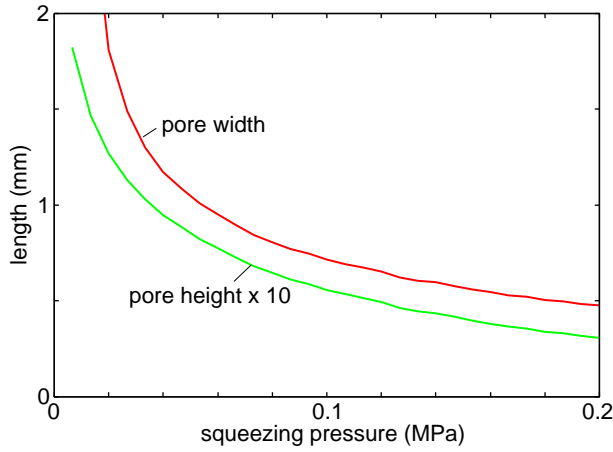


FIG. 9: Calculated critical pore size as a function of the squeezing pressure. For the same system as in Fig. 7.

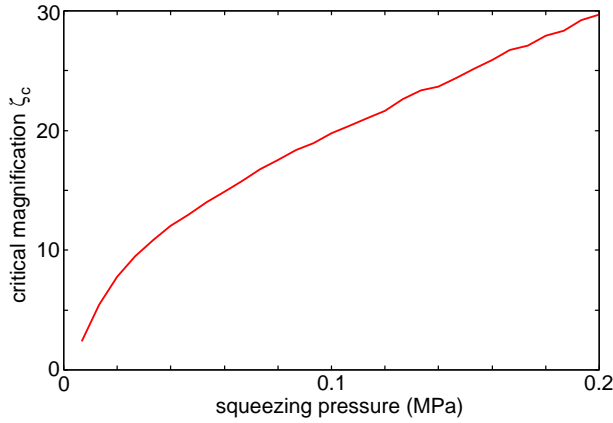


FIG. 10: Calculated critical magnification ζ_c , where the non-contact area percolate, as a function of the squeezing pressure. For the same system as in Fig. 7.

by time and finally no leaking could be observed. But this experiment used unfiltered tap water which contains contamination particles which clogged the channels. We are now using distilled water and find the leak rate (for a given fluid pressure difference) to be practically time independent. But these are still preliminary studies and we will report on the final results elsewhere.

Finally, we note that it is nearly impossible to calculate α theoretically and we have fitted α to reproduce the experimental data. However, this is just one parameter and the dependence of the leak rate on the nominal rubber-countersurface pressure is highly non-trivial and accurately given by the theory. Also, α is of order unity as expected from theory. The only way (as we see it) to obtain a theory-estimate of α would be to generate critical constrictions using numerically exact contact mechanics calculations (e.g., molecular dynamics), and to simulate the fluid flow through the constrictions using numerical methods of fluid flow dynamics.

To summarize, we have compared experimental data with theory for the leak-rate of seals. The theory is based on percolation theory and a recently developed contact mechanics theory. The experiments are for silicon rubber seals in contact with sand paper. The elastic properties of the rubber and the surface topography of the sand paper are fully characterized. The calculated leak-rate \dot{Q} is in good agreement with experiment. The theory only account for fluid flow through the percolation channels observed at (or close to) the percolation threshold. A more accurate treatment should include also flow channels observed at higher magnification. This problem has similarities to current flow in random resistor networks[18, 19].

We thank Christian Schulze (ISAC, RWTH Aachen University) for help with the measurement of the surface topography of the sand paper surfaces. This work, as part of the European Science Foundation EUROCORES Program FANAS, was supported from funds by the DFG and the EC Sixth Framework Program, under contract N ERAS-CT-2003-980409.

-
- [1] R. Flitney, *Seals and sealing handbook* (Elsevier, 2007).
 - [2] M. Mofidi, B. Prakash, B.N.J. Persson and O. Albohr, J. Phys.: Condens. Matter **20**, 085223 (2008).
 - [3] See, e.g., B.N.J. Persson, O. Albohr, U. Tartaglino, A.I. Volokitin and E. Tosatti, J. Phys. Condens. Matter **17**, R1 (2005).
 - [4] B.N.J. Persson, O. Albohr, C. Creton and V. Peveri, J. Chem. Phys. **120**, 8779 (2004)
 - [5] B.N.J. Persson and C. Yang, J. Phys.: Condens. Matter, **20**, 315011 (2008)
 - [6] B.N.J. Persson, J. Chem. Phys. **115**, 3840 (2001).
 - [7] B.N.J. Persson, Phys. Rev. Lett. **99**, 125502 (2007).
 - [8] B.N.J. Persson, Surf. Science Reports **61**, 201 (2006).
 - [9] B.N.J. Persson, Eur. Phys. J. E **8**, 385 (2002).
 - [10] B.N.J. Persson, F. Bucher and B. Chiaia, Phys. Rev. B **65**, 184106 (2002).
 - [11] C. Yang and B.N.J. Persson, J. Phys.: Condens. Matter **20**, 215214 (2008).
 - [12] B.N.J. Persson, J. Phys.: Condens. Matter **20**, 312001 (2008).
 - [13] J.A. Greenwood and J.B.P. Williamson, Proc. Roy. Soc. London A **295**, 300 (1966).
 - [14] A.W. Bush, R.D. Gibson and T.R. Thomas, Wear **35**, 87 (1975).
 - [15] C. Campana, M.H. Müser and M.O. Robbins, J. Phys.: Condens. Matter **20**, 354013 (2008)
 - [16] G. Carbone and F. Bottiglione, J. Mech. Phys. Solids **56**, 2555 (2008).
 - [17] B. Lorenz and B.N.J. Persson, J. Phys.: Condens. Matter **20**, 015003 (2009).
 - [18] D. Stauffer and A. Aharony, *An Introduction to Percolation Theory*, CRC Press (1991).
 - [19] Z. Wu, E. Lopez, S.V. Buldyrev, L.A. Braunstein, S.

Havlin and H.E. Stanley, Phys. Rev. E**71**, 045101(R)
(2005).